2004 ANNUAL REPORT

Broadband Simulation of Ground Motion From Large Earthquakes in the Los Angeles Area Using Stochastic and Deterministic Approaches

Arben Pitarka
Robert Graves
Nancy Collins

URS Group Inc., Pasadena, CA

Introduction

The objective of this study was two-fold. First, to validate our proposed broadband ground motion simulation technique by comparing simulated and recorded ground motions for the Northridge, California earthquake. Second, to produce broadband ground motion time histories on a regular grid of stations covering the Los Angeles area for scenario earthquakes on the Newport-Inglewood fault. In these scenario simulations we used the same fault model parameterizations that were used by the SCEC/ PEER-LL 3D Basin Model Group to estimate 3D ground motion effects in the Los Angeles basin.

Simulation Method

In our broad-band simulations we used the HGF method of Graves and Pitarka (2003). The technique uses a hybrid scheme that combines deterministic and stochastic methods to calculate the low and high frequency parts of the ground motion.

The low frequency simulation methodology uses a deterministic representation of source and wave propagation effects and is based on the approach described by Hartzell (1983). The basic calculation is carried out using a 3D viscoelastic finite-difference algorithm, which incorporates both complex source rupture as well as wave propagation effects with arbitrarily heterogeneous 3D geologic structure (Graves, 1996; Pitarka 1998). The earthquake source is specified by a kinematic description of fault rupture, incorporating spatial heterogeneity in the slip, rupture velocity and rise time. The functional form of the slip velocity time function is based on results of rupture dynamics simulations (e.g. Guaterri et al.,2003). The rise time comes from the empirical model of Somerville et al.(1999), and may vary across the fault. In practice we only allow a depth dependent scaling such that the rise time increases by a factor of 2 if the rupture, ie between 0 and 5 km depth. The rupture time is determined based on the rupture velocity that varies with the shear wave velocity, and is perturbated by a small amount of time that scales linearly with slip amplitude. The scaling results in faster rupture across portions of the fault that have large slip.

The high frequency simulation methodology is a stochastic approach that sums the response for each subfault assuming a random phase, an omega-squared source spectrum and simplified Green's functions. The methodology follows from Boore (1983) with extension to finite-faults given by Frankel (1995). Details of the methodology are described by Graves and Pitarka (2003). Each subfault is allowed to rupture with a subfault moment weighting that is proportional to the final static slip. The final summed moment is than scaled to the prescribed target mainshock moment. The convolution operator of Frankel (1995) scales the subevent rise time to the target rise time. Additionally this operator ensures that the result is not dependent on the choice of the subfault dimensions. Finally we apply amplification functions to the amplitude spectra of the Fourier transformed simulated time histories of both low and high frequency parts in order to correct the simulated ground motion for local site effects. The amplification functions are derived empirically by Borcherdt (1994). In a final step the individual responses are combined into broadband response using a set of matched Butterworth filters.

Validation Study

The broadband procedure described above has been tested against the recorded ground motions of the 1994 Northridge earthquake. We adopted the fault geometry and the final slip distribution of Hartzell et al.(1996) for our simulations. The model region for the simulations covers an area includes 69 strong ground motion recording sites. The subsurface velocity structure used for the deterministic simulations is taken from Version 2 of the SCEC 3D Seismic Velocity Model (Magistrale et al.,2000). Figure 1 compares the data and simulations using the goodness-of-fit measures for 5% damped spectral acceleration calculated from the broadband time histories. The simulation results have no significant bias over the period range of 0.1 to 10 seconds, indicating that the simulation model adequately captures the main characteristics of the ground motion.

Ground Motion Simulation for M6.9 Scenario Earthquakes on the Newport Inglewood Fault.

We generated broad-band (0.1-10 Hz) ground motion time histories on a regular grid of stations covering the Los Angeles area for six M6.9 scenario earthquakes on the Newport-Inglewood fault using the SCEC 3D Velocity Model. The stations are located on a 4km x 4km grid. The location of the study area, stations location and the Newport Inglewood fault are shown in Figure 2. We used the same fault model parameterizations that were used by the SCEC / PEER-LL 3D Basin Model Group to estimate 3D ground motion effects in the Los Angeles basin (SCEC Project Report of the 3D Basin Model Group, 2003). The fault used for these scenarios is based on descriptions from the SCEC Community Fault Model (CFM). Site types range from Vs30 categories A to C. The fault is 50 km long and has a down dip width of 15 km. The fault strike is 106^o, dip is 90^o and the rake averages about 0^o. The fault ruptures the surface. We used a seismic moment of $2.53x10^6$ dyne.cm, giving a moment magnitude of 6.9. Figure 3 shows the final static slip distribution simulated for one of the scenario earthquakes. The hypocenter is in the northern edge of the fault at a depth of about 10 km. The PI was a member of the 3D Basin Model Group and generated some of the ground motion synthetics using a 3D-FDM. For this earthquake we will run two hypocenter locations and three slip models, for a total of six scenarios. We set the lowest shear wave velocity to be 500 m/s in our simulations. With a minimum finite-difference grid spacing of 200 m in the lowest velocity regions we obtain reliable results for frequencies of about 0.5 Hz or less.

For the stochastic simulations we have used the basic 1D profiles for each site. The minimum shear wave velocity is tapered to 760 m/s. For each of the 1600 strong motion sites, site category and Vs^{30} values are obtained from the site condition map for California. We constructed frequency-dependent amplification functions that are applied to the results of the deterministic and stochastic simulations. The final simulated broadband time histories are computed using a pair of match-filters centered at 0.5 Hz.

Figure 4 shows the simulated ground motion at nine selected sites located in the Los Angeles basin and the Santa Monica mountains. The location of the selected station is shown in Figure 2. The simulations demonstrate key phenomena such as the puls-like motions at the forward directivity near-fault stations (g4327 and g4343) and the relatively long duration and lower frequency motions at deep basin sites (g2759). In figure 5 we show maps of average horizontal peak acceleration, and average peak acceleration response at 2 s. Both spatial distributions demonstrate the strong source process effect on the amplitude of near fault motion. The source effect remains predominant over a broad frequency range. Based on our simulations results the ground motion for scenario earthquakes on the Newport Inglewood fault is expected to be relatively large (PGA up to 0.4 g) over a large area of the basin, and along the fault, including San Fernando Valley. The spectral acceleration at 2sec decreases rapidly with the distance from the fault. Because the fault is located close to the deepest part of the basin, the near-fault ground motion amplification is a cumulative effect of both rupture directivity and 3D long period basin response.

The time histories of acceleration at 1600 sites simulated for six M6.9 scenario earthquakes on the Newport Inglewood fault are available upon request. We will work with the SCEC ITR group to associate metadata with the broadband synthetics and make them available for the community through the desired SCEC ITR storage and distribution systems.

References

3D Basin Model Group (2003). 3D Ground Motion Simulation in Basins, SCEC Annual Report, 2003.

Graves, R.W. and A. Pitarka (2004). Broadand time history simulation using a hybrid approach, *Proc. 13th World Conf. Earthquake Eng., Vancouver, Canada*, paper no. 1098.

Beroza, C.G. amd M. Guatteri (2003). Physically based source input for strong ground motion simulation. PEER Lifelines Final Report : Project 1C08

Borcherdt R. (1994). Estimates of site-dependent response spectra for design (methodology and justification). Earthquake Spectra. 10(4), 617-653.

Boore, D.M. (1983). Stochastic simulation of high-frequency ground motions based on seismological models of the radiated spectra, Bull. Seism. Soc. Am., 73, 1865-1894.

Frankel, A. (1995). Simulating strong motion of large earthquakes using recordings of small earthquakes: the Loma Prieta Mainshock as a test case, Bull. Seism. Soc. Am., 85, 1144-1160.

Guatteri, M, P.M. Mai, and G. C. Beroza (2003). A recipe to generate physically consistent earthquake rupture models for ground motion predictions (submitted to BSSA)

Pitarka, A (1999). 3D elastic finite-difference modeling of seismic motion using staggered grids with nonuniform spacing. BSSA, 89, 54-68.

Pitarka A., P. Somerville, Y. Fukushima, T. Uetake, and K.Irikura (2000). Simulation of near-fault-strong ground motion using hybrid Greens functions, BSSA, 90,566-586.

Hartzell S, Heaton T. (1983). Inversion of strong ground motion and teleseismic waveform data for the fault rupture history of the 1979 Imperial Valley, California earthquake. BSSA, 73, 1553-1583.

Hartzell et al. (1996). The 1994 Northridge, California earthquake: Investigation of rupture velocity, rise time, and high frequency radiation. J.Geophys.Res. 101, 20091-20108.

Pitarka,A.(1998). 3D elastic finite-difference modeling of seismic wave propagation using staggered grid with non-uniform spcing, BSSA,88,54-68.

Graves,R. (1996). Simulating seismic wave propagation in 3D elastic media using staggered grid finite differences. BSSA, 86, 1091-1106.

Somerville et al. (1999). Characterizing crustal earthquake slip models for the prediction of the strong ground motion. Seism.Res. Lett.70,59-80.

Magistrale et al. (2000) The SCEC Southern California reference three-dimensional seismic velocity model version 2. BSSA. 90(6b),S77-S94.

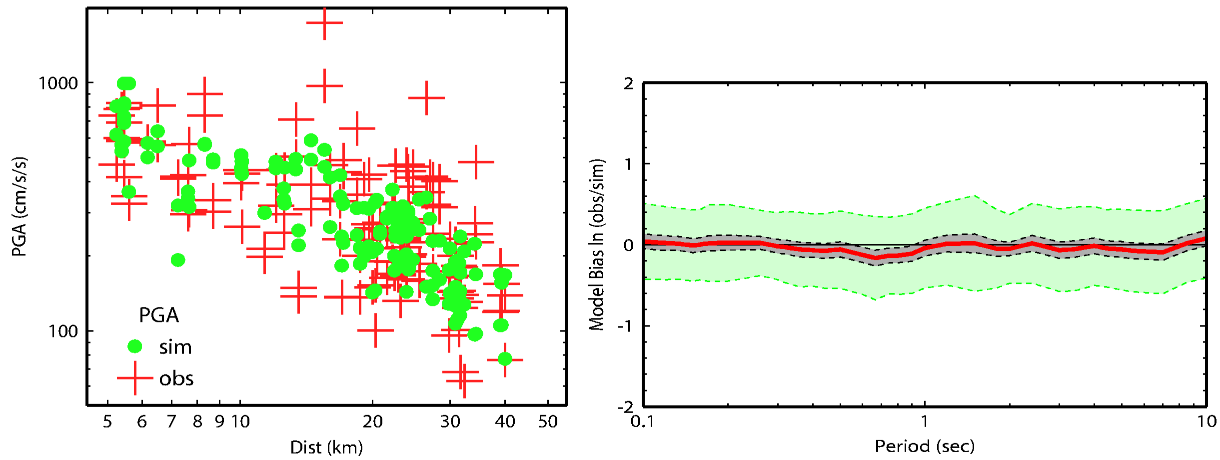

Figure 1. Left. Observed (red crosses) and simulated (green circles) peak ground acceleration plotted as afunction of closest distance to fault at 69 sites for the Northridge earthquake.

Right. Spectral acceleration goodness-of fit computed for the average of both horizontal components for the Northridge earthquake.

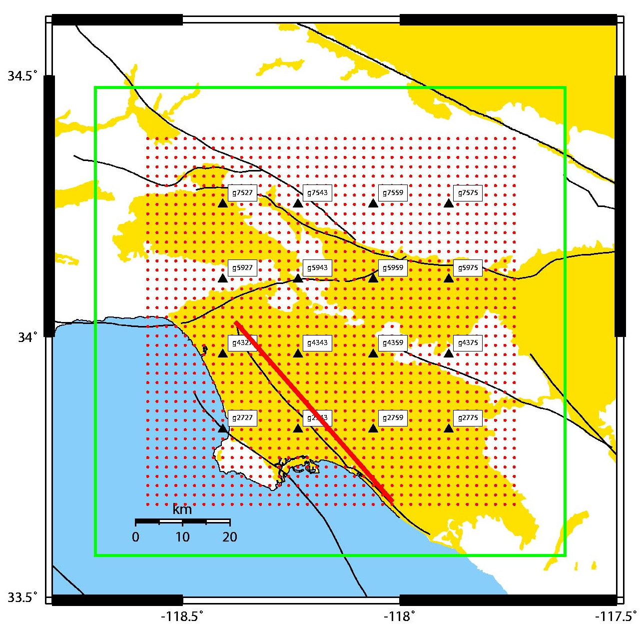

Figure 2. Map of the region used in the broad-band simulation of the ground motion from the M6.9 Newport Inglewood scenario earthquake. Red line indicates the fault location. Red dots indicate the sites location used in the simulations.

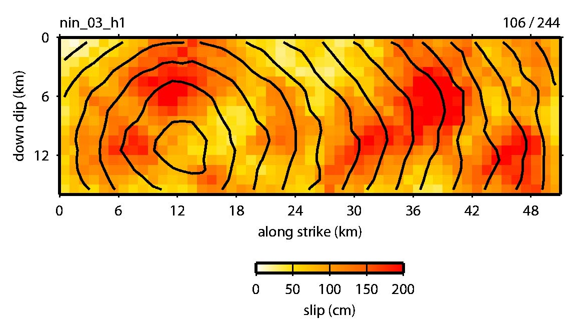

Figure 3. Slip distribution of the Newport-Inglewood scenario earthquake. Contours show rupture front at 1 sec intervals.

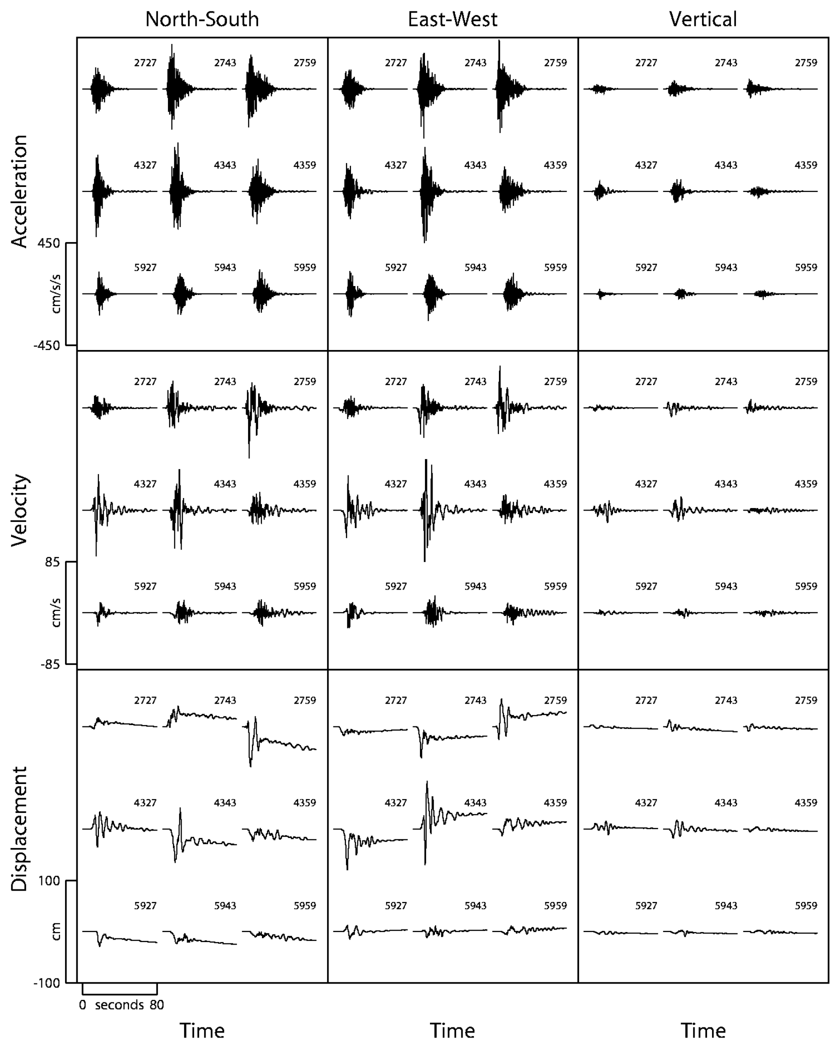

Figure 4. Simulated time histories of ground motion acceleration, velocity and displacement at selected stations. The stations name is indicated at the top of each trace. The stations location is shown by rectangles in Figure 3.

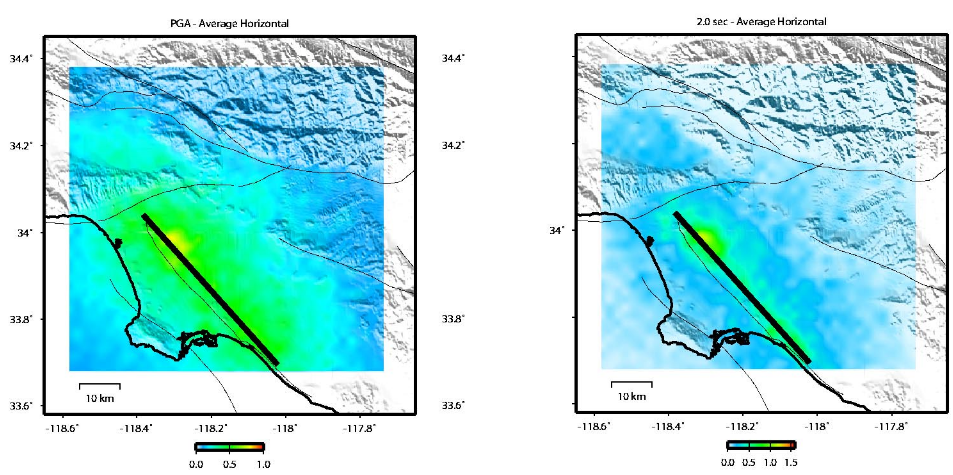

Figure 5. Map of the simulated average horizontal peak acceleration (left) and spectral acceleration at 2 sec period

(right) for the M6.9 Newport-Inglewood scenario earthquake.